# All-electron first-principles investigations of the energetics of vicinal Cu surfaces

Juarez L. F. Da Silva,[1,*] Cyrille Barreteau,[2] Kurt Schroeder,[1] and Stefan Blügel[1]
[1]*Institut für Festkörperforschung, Forschungszentrum Jülich, D-52425 Jülich, Germany*
[2]*DSM/DRECAM/SPCSI, CEA Saclay, F-91191 Gif Sur Yvette, France*
(Received 28 September 2005; revised manuscript received 13 January 2006; published 7 March 2006)

Using first-principles calculations we studied the energetics (surface energy, step energy, stability with respect to faceting) of the low- and high-Miller-index (vicinal) Cu surfaces, namely, the (111), (100), (110), (311), (331), (210), (211), (511), (221), (711), (320), (553), (410), (911), and (332) surfaces. Our calculations are based on density-functional theory employing the all-electron full-potential linearized augmented plane-wave (FLAPW) method. We found that the unrelaxed vicinal Cu surfaces between (100) and (111) are unstable relative to faceting at 0 K, while fully relaxed vicinal surfaces between (100) and (111) are stable relative to faceting, which is in agreement with the observed stability of vicinal Cu surfaces at room temperature. Thus atomic relaxations play an important role in the stability of the vicinal Cu surfaces. Using the surface energies of Cu(111), Cu(100), and Cu(110) and employing the effective pair-potential model, which takes into account only the changes in the coordination of the surface atoms, the surface energies of the vicinal Cu surfaces can be calculated with errors smaller than 1.0% compared with the calculated FLAPW surface energies. This result is due to the *almost perfect* linear scaling of the surface energies of the Cu(*hkl*) surfaces as a function of the total number of broken nearest-neighbor bonds. Furthermore, we calculate step-step interactions as a function of terrace widths and step energies of isolated steps.

DOI: 10.1103/PhysRevB.73.125402 PACS number(s): 68.35.Bs, 68.35.Md, 71.15.Ap

## I. INTRODUCTION

The surface energy of a solid metal surface is an important physical property which plays a role in determining the equilibrium shape of crystals, stability of vicinal metal surfaces with respect faceting, etc. Hence it contributes to determine the behavior of solid metal surfaces when used in various technological applications such as catalysis, electrochemistry, corrosion, and lubrication.[1] Direct experimental measurements of the absolute value of the surface energy are difficult to perform and are subject to various uncertainties, e.g., presence of impurities. However, recent advances in experimental techniques have been made in the last years. Métois and Müller[2] proposed a simple method to obtain the absolute value of the surface energy of a given solid system, which is based on two independent measurements on three-dimensional (3D) and 2D equilibrium shapes completed by the analysis of the thermal fluctuation of an isolated step. Furthermore, Bonzel and Edmundts[3] showed that analyzing the 3D equilibrium crystal shapes of crystallites for a wide range of temperatures by scanning tunneling microscopy (STM) can yield absolute values of the surface and step energies versus temperature. This technique was applied for Pb surfaces, namely, (111), (100), (110), (311), (112), and (221).[4,5] These experimental techniques can provide the orientation dependence of the surface energy, as well as the step-step interactions and kink energies.[6,7] However, most of the available experimental surface energy data were obtained from surface tension measurements in the liquid phase and extrapolated to zero temperature.[1,8,9] Hence it cannot provide the anisotropy of the surface energy.

Due to the difficulties in obtaining highly precise experimental surface energies and the surface orientation dependence, theoretical calculations have played a key role in calculating the absolute value of the surface energy for different orientations.[11–27] For example, Methfessel *et al.*,[11] employing the full-potential linear muffin-tin orbital (FP-LMTO) method, found a roughly parabolic behavior for the surface energy of the low-Miller-index (flat) surfaces across the 4*d* transition-metal series, which was explained in terms of the *d*-band occupation. Almost at the same time, Skriver and Rosengaard,[12] employing a Green's-function technique based on the LMTO method, discussed the trends exhibited by the surface energies of flat surfaces of the alkali, alkaline earth, divalent rare-earth, 3*d*, 4*d*, and 5*d* transition and noble metals, as derived from the surface tension of liquid metals. Furthermore, Vitos *et al.*,[19] using a full-charge Green's-function LMTO approach, elaborated a useful database that contains the surface energy for 60 flat metal surfaces in the periodic table. Recently, Galanakis *et al.*,[23,24] employing the full-potential screened Korringa-Kohn-Rostoker (FKKR) method, obtained in good approximation that the energy to create a surface for the Cu, Ag, and Au metals depends only on the number of broken nearest-neighbor bonds and not on the cleavage plane, which is known as the broken-bond rule.

The studies mentioned above yielded a real improvement in the understanding of the surface energy trends, however, most of these studies were mainly restricted to the study of flat surfaces, except the work performed by Galanakis and co-workers,[23,24] in which three unrelaxed vicinal surfaces were calculated. The study of the energetics of high-Miller-index (stepped, vicinal) surfaces is essential to the understanding of various surface properties such as the equilibrium shape of crystals, crystal growth, surface morphology, step-step interactions, kink energies, stability with respect faceting, etc.[1] Recently, different theoretical approaches have been used to study the stability of vicinal metal surfaces with respect to faceting.[20,22] Frenken and Stoltze,[20] using the effective-medium theory (EMT), predicted that most vicinal surfaces are unstable relative to faceting at 0 K and claimed

 

TABLE I. Computational parameters used in the surface energy calculations of the low- and high-Miller-index Cu($hkl$) surfaces. In the terrace-step notation $[p(h'k'l')\times(uvw)]$ $(h'k'l')$ and $(uvw)$ indicate the terrace and step orientations, while $p$ indicates the number of atom rows in the terrace. $|\vec{a}|$ and $|\vec{b}|$ are the dimensions of the $(1\times1)$ surface unit cell, while $\omega$ is the angle between the vectors $\vec{a}$ and $\vec{b}$. The area of the $(1\times1)$ surface unit cell are indicated in the sixth column, while $d_0$ is the interlayer spacing distance between two adjacent surface layers parallel to the ($hkl$) surface. $N_{\text{slab}}$ indicate the number of layers in the slab used to model the Cu($hkl$) surface, while the slab thickness is given by $D=(N_l-1)d_0$. The last two columns indicate the two-dimensional Monkhorst-Pack **k** point grids and the respective number of **k** points in the irreducible part of the surface BZ (IBZ), respectively. The equilibrium theoretical Cu lattice constant is 3.63 Å.

| Surface | $p(h'k'l')\times(uvw)$ | $\lvert\vec{a}\rvert/a_0$ | $\lvert\vec{b}\rvert/a_0$ | $\omega$ | Area (Å$^2$) | $d_0$ (Å) | $N_{\text{slab}}$ | $D$ (Å) | **k** mesh | $N_{\mathbf{k}}^{IBZ}$ |
|---|---|---|---|---|---|---|---|---|---|---|
| Cu(111) | | $\sqrt{2}/2$ | $\sqrt{2}/2$ | 120° | 5.704 | $a_0/\sqrt{3}=2.096$ | 7 | 12.576 | $(20\times20)$ | 200 |
| Cu(100) | | $\sqrt{2}/2$ | $\sqrt{2}/2$ | 90° | 6.587 | $a_0/\sqrt{4}=1.815$ | 8 | 12.705 | $(20\times20)$ | 200 |
| Cu(110) | | $\sqrt{2}/2$ | 1 | 90° | 9.315 | $a_0/\sqrt{8}=1.283$ | 11 | 12.830 | $(20\times14)$ | 140 |
| Cu(311) | $2(100)\times(111)$ | $\sqrt{2}/2$ | $\sqrt{6}/2$ | 106.779° | 10.923 | $a_0/\sqrt{11}=1.094$ | 13 | 13.128 | $(20\times12)$ | 120 |
| Cu(331) | $3(111)\times(11\bar{1})$ | $\sqrt{2}/2$ | $\sqrt{10}/2$ | 102.921° | 14.356 | $a_0/\sqrt{19}=0.833$ | 17 | 13.328 | $(20\times9)$ | 90 |
| Cu(210) | $2(110)\times(100)$ | 1 | $\sqrt{6}/2$ | 114.095° | 14.729 | $a_0/\sqrt{20}=0.816$ | 17 | 13.056 | $(14\times11)$ | 77 |
| Cu(211) | $3(111)\times(100)$ | $\sqrt{2}/2$ | $\sqrt{12}/2$ | 90° | 16.135 | $a_0/\sqrt{24}=0.741$ | 19 | 13.338 | $(20\times8)$ | 80 |
| Cu(511) | $3(100)\times(111)$ | $\sqrt{2}/2$ | $\sqrt{14}/2$ | 100.893° | 17.113 | $a_0/\sqrt{27}=0.699$ | 19 | 12.582 | $(20\times8)$ | 80 |
| Cu(331) | $4(111)\times(11\bar{1})$ | $\sqrt{2}/2$ | $\sqrt{18}/2$ | 90° | 19.761 | $a_0/\sqrt{36}=0.605$ | 23 | 13.310 | $(20\times7)$ | 70 |
| Cu(711) | $4(100)\times(111)$ | $\sqrt{2}/2$ | $\sqrt{26}/2$ | 97.971° | 23.520 | $a_0/\sqrt{51}=0.508$ | 27 | 13.208 | $(20\times6)$ | 60 |
| Cu(320) | $3(110)\times(100)$ | 1 | $\sqrt{14}/2$ | 105.501° | 23.749 | $a_0/\sqrt{52}=0.503$ | 27 | 13.078 | $(14\times7)$ | 49 |
| Cu(331) | $5(111)\times(11\bar{1})$ | $\sqrt{2}/2$ | $\sqrt{30}/2$ | 97.418° | 25.298 | $a_0/\sqrt{59}=0.473$ | 29 | 13.231 | $(20\times5)$ | 50 |
| Cu(410) | $4(100)\times(110)$ | 1 | $\sqrt{18}/2$ | 103.633° | 27.159 | $a_0/\sqrt{68}=0.440$ | 31 | 13.200 | $(14\times7)$ | 49 |
| Cu(911) | $5(100)\times(111)$ | $\sqrt{2}/2$ | $\sqrt{42}/2$ | 96.264° | 30.005 | $a_0/\sqrt{83}=0.398$ | 33 | 12.736 | $(20\times4)$ | 40 |
| Cu(332) | $6(111)\times(11\bar{1})$ | $\sqrt{2}/2$ | $\sqrt{44}/2$ | 90° | 30.895 | $a_0/\sqrt{88}=0.387$ | 35 | 13.155 | $(20\times4)$ | 40 |

that the observed stability at room temperature arises from the entropic contributions due to thermal vibrations. However, Desjonquères *et al.*[22] proved that for a wide class of empirical potentials all vicinal surfaces between (100) and (111) are unstable at 0 K, moreover, thermal vibrations do not play a crucial role in the delicate energy balance which drives the stability. Therefore a clear and simple explanation for the observed stability of vicinal metal surfaces with respect to faceting is still missing.

To obtain a clear understanding of the stability of the vicinal Cu surfaces with respect to faceting at 0 K, which is still missing in the literature, as well as to contribute to the understanding of the surface energy trends with respect to surface orientation, we performed systematic density-functional theory (DFT) calculations employing the all-electron full-potential linearized augmented plane-wave (FLAPW) method for fifteen Cu surfaces: (111), (100), (110), (311), (331), (210), (211), (511), (221), (711), (320), (553), (410), (911), (332). Furthermore, using our FLAPW surface energies, we will discuss the accuracy of the effective pair-potential model to estimate the surface energy of vicinal Cu surfaces, step energies of isolated steps, and stability of vicinal surfaces with respect faceting at 0 K.

The remainder of this paper is organized as follows: In Sec. II, the theoretical approach will be described. In Sec. III, the results are presented and discussed. Sec. IV summarizes the main conclusions obtained in the present work. Some technical details are discussed in the Appendix.

## II. METHOD AND COMPUTATIONAL DETAILS

Our calculations are based on DFT,[28,29] within the generalized gradient approximation.[30] The Kohn-Sham equations are solved using the all-electron FLAPW method[31] as implemented in the FLEUR code,[32] in which the solid surfaces are modeled using the film geometry, i.e., a single slab is sandwiched between two semi-infinite vacua.[33] The LAPWs wave functions in the interstitial region are represented using a plane-wave expansion truncated to include only plane waves that have kinetic energies less than $K^{wf}=18.06$ Ry,[34] and for the potential representation in the interstitial region, plane waves up to $G^{pot}=273$ Ry are considered. Inside the muffin-tin spheres with radius $R_{mt}=1.16$ Å, the wave functions are expanded in radial functions times spherical harmonics up to $l_{max}=9$, and for the potential a maximum of $\tilde{l}_{max}=9$ is also used. For the evaluation of the nonspherical matrix elements of the Hamiltonian we include terms up to $l_{max}^{ns}=6$.

Integrations over the surface Brillouin zone (BZ) were performed using a two-dimensional Monkhorst-Pack[35]

TABLE II. Surface energy of Cu surfaces as a function of the number of layers in the slab, $N_{slab}$. $E^f_{surf}$ and $E_{surf}$ indicate the surface energies per surface atom of unrelaxed and fully relaxed slabs, respectively.

| $N_{slab}$ | $E^f_{surf}(111)$ (eV) | $E_{surf}(111)$ (eV) | $N_{slab}$ | $E^f_{surf}(100)$ (eV) | $E_{surf}(100)$ (eV) | $N_{slab}$ | $E^f_{surf}(110)$ (eV) | $E_{surf}(110)$ (eV) | $N_{slab}$ | $E^f_{surf}(311)$ (eV) | $E_{surf}(311)$ (eV) |
|---|---|---|---|---|---|---|---|---|---|---|---|
| 3 | 0.468 | 0.466 | 4 | 0.613 | 0.609 | 7 | 0.920 | 0.896 | 9 | 1.093 | 1.063 |
| 5 | 0.467 | 0.467 | 6 | 0.607 | 0.602 | 9 | 0.917 | 0.894 | 11 | 1.096 | 1.067 |
| 7 | 0.470 | 0.469 | 8 | 0.608 | 0.603 | 11 | 0.925 | 0.901 | 13 | 1.093 | 1.063 |
| 9 | 0.469 | 0.468 | 10 | 0.608 | 0.602 | 13 | 0.923 | 0.898 | 15 | 1.093 | 1.064 |
| 11 | 0.469 | 0.468 | 12 | 0.606 | 0.600 | 15 | 0.925 | 0.901 | 17 | 1.087 | 1.059 |

**k** mesh with the broadening of the Fermi surface by the Fermi-Dirac distribution function ($k_B T_{ele}$=54 meV). The total energy was extrapolated to zero temperature.[36] The **k** meshes and the corresponding number of **k** points in the surface BZ are summarized in Table I. The theoretical equilibrium lattice constant (3.63 Å), which is in good agreement with experiment results,[37] was used in our calculations.[38] The low- and high-Miller-index Cu surfaces are modeled using a $(1\times1)$ surface unit cell, in which there is one Cu atom per atomic layer. The most important geometric parameters of the surface unit cells are summarized in Table I. Furthermore, the vicinal Cu surfaces are presented in Table I using also the terrace-step notation.[39] All layers in the slab were allowed to relax and the equilibrium configuration is assumed when the atomic force on each atom is smaller than 0.50 mRy/bohr. The multilayer relaxations of the studied Cu surfaces, as well as further technical details, are discussed elsewhere.[40–42]

## III. RESULTS AND DISCUSSION

The surface energy $E_{surf}$ is defined as the energy (per surface atom or per unit area) needed to split an infinite crystal into two semi-infinite crystals along some chosen plane.[1] The Cu surfaces are modeled using a single slab with a finite number of layers, $N_{slab}$. Using this approach, $E_{surf}$ is given by

$$E_{surf} = \frac{1}{2}(E^{slab}_{tot} - N_{slab}E^{bulk}_{tot}), \quad (1)$$

where $E^{slab}_{tot}$ is the total energy of a slab with $N_{slab}$ layers (one atom per atomic layer), while $E^{bulk}_{tot}$ is the reference bulk total energy per atom. The factor 1/2 takes into account that the slab is bounded by two equivalent surfaces. Thus $E_{surf}$ is a function of the number of layers in the slab, and hence surface energies calculated using Eq. (1) can be compared with experimental surface energies obtained from semi-infinite films only in the asymptotic regime (large values of $N_{slab}$). The central problem in calculating accurate surface energies using first-principles calculations is to obtain a reliable value for $E^{bulk}_{tot}$. For example, an error of 10 meV in the reference bulk total energy introduces an error of 0.165 eV (using $N_{slab}$=33) in the surface energy of the Cu(911) surface. Therefore surface energy calculations, as well as the physical quantities derived from the surface energies such as step energies, relative stability, etc., require highly accurate bulk and slab total-energy calculations.

In principle, the required total energies in Eq. (1) can be calculated from two separated self-consistent calculations (slab and bulk) using the same theoretical approach. However, FP-LMTO calculations found that the surface energy of Pt(100) calculated from two separated self-consistent calculations decrease as a function of the number of layers in the slab, which is an unphysical and unexpected result.[43] This problem was recently discussed by Da Silva[38] employing the FLAPW method[44] and the repeated slab geometry. It was found that the surface energy of Cu(111) calculated from two separated self-consistent calculations and using Eq. (1) converges as a function of the number of layers in the slab. Unconverged calculations with respect to the number of **k** points determines the divergent behavior of $E_{surf}$ as a function of the number of layers in the slab. Da Silva[38] pointed out that similar high quality integrations over the surface and bulk BZ are required to obtain converged surface energies, which is only obtained by using high dense **k**-point meshes in both calculations, e.g., $(20\times20)$ for Cu(111). Furthermore, the slab and bulk systems need to be treated using exactly the same basis function type and cutoff energies.

In the present work, the Cu surfaces are modeled using the single slab geometry.[33] Thus the semi-infinite vacua on both sides of the single slab are described by plane waves times exponential decay functions, which are not used in the description of the bulk system. Hence the bulk and slab systems are not treated exactly with the same basis function type. Thus the reference bulk total energy required in Eq. (1) has to be obtained using a different approach. In the limit of large values of $N_{slab}$, the reference bulk total energy can be obtained by a linear fit of the slab total energies,[43] which was used in the present work to obtain $E^{bulk}_{tot}$. Calculations were performed for the unrelaxed (111), (100), (110), and (311) surfaces using different numbers of layers in the slab, from which $E^{bulk}_{tot}$ was extracted by a linear fitting. The same approach was successfully used to study the dependence of the surface energy of the flat Al surfaces as a function of the number of layers in the slab.[27]

The surface energies of the unrelaxed and relaxed (111), (100), (110), (311) Cu surfaces as a function of $N_{slab}$ are summarized in Table II. We found that well converged surface energies for (111), (100), (110), (311) can be obtained using 7 (1 meV), 8 (2 meV), 11 (0 meV), and 13 (6 meV) layers in the slab, respectively, which corresponds to slab thickness of 12.58, 12.71, 12.83, and 13.13 Å, respectively. The number in parentheses indicate the difference with respect calculations using 11, 12, 15, and 17 layers for (111),

TABLE III. Surface energy of low- and high-Miller-index Cu(*hkl*) surfaces. $E^f_{surf}$ and $E_{surf}$ indicate the surface energy per surface atom of unrelaxed and fully relaxed slabs, respectively. $\Delta E_{surf}$ indicates the change in the surface energy due to the multilayer relaxations ($\Delta E_{surf}=E^f_{surf}-E_{surf}$). $E^{\star,f}_{surf}$ and $E^{\star}_{surf}$ indicates the surface energy anisotropy ratios [$E^{\star}_{surf}=E_{surf}(hkl)/E_{surf}(111)$] calculated from the surface energies given in electron volt per surface atom of unrelaxed and fully relaxed slabs, respectively. $N_b$ indicates the total number of broken nearest-neighbor bonds in the Cu(*hkl*) surface. $N^{\star}_b$ indicates the anisotropy ratios calculated from the total number of broken nearest-neighbor bonds [$N^{\star}_b(hkl)=N_b(hkl)/N_b(111)$]. The numbers in parentheses indicate the difference in percent of the surface energy anisotropy ratios with respect to the $N^{\star}_b$ results.

| Surface | $E^f_{surf}$ (eV) | $E_{surf}$ (eV) | $\Delta E_{surf}$ (meV) | $E^f_{surf}/N_b$ (eV) | $E_{surf}/N_b$ (eV) | $E^f_{surf}$ (J/m$^2$) | $E_{surf}$ (J/m$^2$) | $E^{\star,f}_{surf}$ | $E^{\star}_{surf}$ | $N_b$ | $N^{\star}_b$ |
|---|---|---|---|---|---|---|---|---|---|---|---|
| Cu(111) | 0.470 | 0.469 | 0.97 | 0.157 | 0.156 | 1.320 | 1.317 | | | 3 | |
| Cu(100) | 0.608 | 0.603 | 5.24 | 0.152 | 0.151 | 1.479 | 1.466 | 1.294 (−2.95%) | 1.286 (−3.53%) | 4 | 1.333 |
| Cu(110) | 0.925 | 0.901 | 23.67 | 0.154 | 0.150 | 1.591 | 1.550 | 1.969 (−1.55%) | 1.922 (−3.90%) | 6 | 2 |
| Cu(311) | 1.093 | 1.063 | 29.96 | 0.156 | 0.152 | 1.602 | 1.559 | 2.325 (−0.34%) | 2.266 (−2.87%) | 7 | 2.333 |
| Cu(331) | 1.398 | 1.364 | 34.03 | 0.155 | 0.152 | 1.560 | 1.522 | 2.974 (−0.87%) | 2.908 (−3.07%) | 9 | 3 |
| Cu(210) | 1.542 | 1.492 | 49.26 | 0.154 | 0.149 | 1.677 | 1.623 | 3.281 (−1.56%) | 3.182 (−4.53%) | 10 | 3.333 |
| Cu(211) | 1.559 | 1.524 | 35.09 | 0.156 | 0.152 | 1.548 | 1.513 | 3.319 (−0.42%) | 3.251 (−2.46%) | 10 | 3.333 |
| Cu(511) | 1.692 | 1.653 | 39.44 | 0.154 | 0.150 | 1.584 | 1.547 | 3.602 (−1.76%) | 3.525 (−3.86%) | 11 | 3.667 |
| Cu(221) | 1.864 | 1.828 | 35.22 | 0.155 | 0.152 | 1.511 | 1.482 | 3.966 (−0.85%) | 3.899 (−2.53%) | 12 | 4 |
| Cu(711) | 2.306 | 2.261 | 44.93 | 0.154 | 0.151 | 1.571 | 1.540 | 4.907 (−1.96%) | 4.821 (−3.58%) | 15 | 5 |
| Cu(320) | 2.458 | 2.388 | 70.22 | 0.154 | 0.149 | 1.658 | 1.611 | 5.232 (−1.89%) | 5.093 (−4.50%) | 16 | 5.333 |
| Cu(553) | 2.340 | 2.300 | 40.01 | 0.156 | 0.153 | 1.482 | 1.456 | 4.979 (−0.42%) | 4.904 (−1.92%) | 15 | 5 |
| Cu(410) | 2.755 | 2.688 | 67.03 | 0.153 | 0.149 | 1.625 | 1.585 | 5.862 (−2.30%) | 5.731 (−4.48%) | 18 | 6 |
| Cu(911) | 2.928 | 2.877 | 51.56 | 0.154 | 0.151 | 1.563 | 1.536 | 6.232 (−1.59%) | 6.135 (−3.13%) | 19 | 6.333 |
| Cu(332) | 2.806 | 2.765 | 41.03 | 0.156 | 0.154 | 1.455 | 1.434 | 5.971 (−0.48%) | 5.896 (−1.73%) | 18 | 6 |

(100), (110), and (311), respectively. The small variation of the surface energies of (111) and (100) with $N_{slab}$ is due to the small quantum-size effects present in these systems compared with other systems, e.g., Al(111).[27] Based on the present results, all surface energy calculations of the Cu surfaces were performed using a slab thickness of at least 12.50 Å. The exact number of layers used to model the Cu(*hlk*) surfaces are summarized in Table I along with the unrelaxed interlayer and registry distances. All surface energy results are summarized in Table III. Furthermore, the energy gain due to the multilayer relaxations, the surface energy per number of broken nearest-neighbor bonds, and the anisotropy ratios are also summarized in Table III. The few available experimental results and previous theoretical results are summarized in Table IV.

Our results show that the multilayer relaxation decreases the surface energy per surface atom by few percent, e.g., 1.48% for Cu(332). The energy gain due the multilayer relaxations [$\Delta E_{surf}=E^f_{surf}-E_{surf}$] increases with increasing the openness of the surfaces, e.g., $\Delta E_{surf}$ is larger for (410), (320), and (210), which are vicinal surfaces with Cu atoms below the terrace exposed to the vacuum region.[41]

We want to point out the large discrepancies between our results and particular theoretical calculations (see Table IV). Some of these discrepancies are due to the differences between the LDA and GGA functionals, however, in particular cases, approximations in the potentials play a major role in these discrepancies. For example, Da Silva[38] employing the FLAPW method, as implemented in the WIEN code,[44] obtained surface energies of 0.64 eV/atom and 0.50 eV/atom employing the LDA and PBE functionals, respectively, for (111), i.e., a difference of only 0.14 eV/atom due to the LDA and GGA functionals. The surface energy calculated for (111) in the present work (0.47 eV/atom) differs only 0.03 eV/atom from the value obtained by Da Silva[38] employing a different implementation of the FLAPW method and employing the repeated slab geometry.

Our surfaces energies are close to the experimental results reported in Refs. 8 and 9. However, it should be taken into account that these results were obtained using measurements in liquid phase and extrapolated to zero temperature, i.e., an average value over a large number of orientations. However, there are large differences between our results and those experimental results obtained by Bonzel and Nowicki[5] for (111) and (100). It was pointed out in Ref. 5 that assuming a higher vibrational entropy term to compute the step free energies at a temperature of 1240 K improves the agreement with previously published data. The higher vibrational entropy was justified by an increasing importance of anharmonicity at high temperatures.

### A. Broken-bond rule

Using our surface energies given in electron volt per surface atom (see Table III), we calculated the surface energy anisotropy ratios [$E^{\star}_{surf}(hkl)=E_{surf}(hkl)/E_{surf}(111)$]. Furthermore, for comparison, we calculated the broken nearest-neighbor bonds anisotropy ratios [$N^{\star}_b(hkl)=N_b(hkl)/N_b(111)$], where $N_b(hkl)$ indicates the total number of broken nearest-neighbor bonds in the Cu(*hkl*) surface taken into account all surface layers. For the studied Cu surfaces, $N_b(hkl)$ is given by

TABLE IV. Surface energies available in the literature for the low-Miller-index Cu surfaces.

| | Cu(111) | | Cu(100) | | Cu(110) | |
|---|---|---|---|---|---|---|
| | (eV) | ($J/m^2$) | (eV) | ($J/m^2$) | (eV) | ($J/m^2$) |
| FKKR[a] | 0.675 | | 0.874 | | 1.327 | |
| FLAPW[a] | 0.62 | | 0.81 | | 1.25 | |
| LMTO[b] | 0.69 | 1.96 | 0.85 | 2.09 | 1.33 | 2.31 |
| LMTO[c] | 0.707 | 1.952 | 0.906 | 2.166 | 1.323 | 2.237 |
| FLAPW[d] | 0.64 | 1.92 | | | | |
| FLAPW[e] | 0.50 | 1.41 | | | | |
| PP[f] | | 1.585 | | 1.712 | | 1.846 |
| EAM[g] | | 1.181 | | 1.288 | | |
| TB[h] | 0.581 | | 0.748 | | 1.121 | |
| Exp.[i] | | 1.790 | | | | |
| Exp.[j] | | 1.825 | | | | |
| Exp.[k] | | 4.0 | | 5.5 | | |

[a]Reference 23; LDA calculations.
[b]Reference 12; LDA calculations.
[c]Reference 21; GGA calculations.
[d]Reference 38; LDA calculations.
[e]Reference 38; PBE calculations.
[f]Reference 13; pseudopotential LDA calculations.
[g]Reference 14.
[h]Reference 25.
[i]Reference 8; experimental results.
[j]Reference 9; experimental results.
[k]Reference 5; experimental results.

$$N_b(hkl) = \begin{cases} 2h+k & h,k,l \text{ odd} \\ 4h+2k & \text{otherwise} \end{cases} \qquad h \geq k \geq l. \qquad (2)$$

The anisotropy ratios are summarized in Table III. To help in the discussion, we plot the surface energy versus the number of broken bonds in Fig. 1.

There is an excellent agreement between $E^{\star,f}_{\text{surf}}$, $E^{\star}_{\text{surf}}$, and $N^{\star}_b$ for all studied Cu surfaces. The differences are smaller than 3.0% (unrelaxed) and 5.0% (fully relaxed) for all studied Cu surfaces. The surface energies show an *almost perfect* linear scaling as a function of the total number of broken nearest-neighbor bonds for all studied Cu surfaces (see Fig. 1). For example, the surface energy per number of broken nearest-neighbor bonds is *almost constant* for all studied Cu surfaces (see Table III). Thus in a first approximation the surface energy of a particular Cu surface can be estimated using the surface energy of Cu(111) and the number of broken nearest-neighbor bonds. This trend is called the broken-bond rule, which was also obtained by Galanakis and co-workers[23,24] using first-principles calculations for Cu, Ag, and Au surfaces. We found that the broken-bond rule is slightly better respected on a fixed lattice than when the atomic positions are allowed to relax. This can be attributed to the fact that in the relaxed system many different inequivalent bonds will appear corresponding to local changes of the first neighbor Cu-Cu distances.[40–42]

The surface energy anisotropy ratios obtained by Galanakis and co-workers[23,24] are closer to the ideal values, i.e., $N^{\star}_b$, than our results. By investigating the behavior of the anisotropy ratios as a function of the computational parameters, we found that the surface energy anisotropy ratios depends on the cutoff energy and of the number of **k** points in the irreducible part of the BZ. Relatively small cutoff energies, e.g., 10.56 Ry, provided anisotropy ratios closer to the

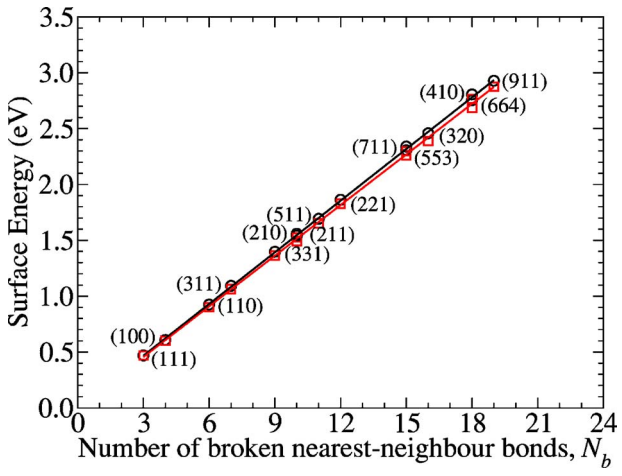


FIG. 1. (Color online) Surface energy of low- and high-Miller-index Cu surfaces versus the number of broken nearest-neighbor bonds in the surface, $N_b$. Circles (in black) and squares (in red) indicate surface energies of unrelaxed and fully relaxed surfaces, respectively. The continuous lines are obtained from a linear fitting of the surface energy DFT results.

TABLE V. Effective pair-potential (EPP) parameters calculated from the surface energies of the low-Miller-index Cu surfaces (see the Appendix). The EPP parameters are given in electron volts.

| | Unrelaxed slabs | | | Relaxed slabs | | |
|---|---|---|---|---|---|---|
| Method | $V_1^f$ | $V_2^f$ | $V_3^f$ | $V_1$ | $V_2$ | $V_3$ |
| FLAPW[a] | +0.151 | +0.009 | −0.001 | +0.131 | +0.011 | +0.004 |
| FLAPW[b] | +0.225 | +0.008 | −0.007 | | | |
| FKKR[b] | +0.225 | +0.012 | −0.003 | | | |
| LMTO[c] | +0.163 | +0.018 | +0.014 | | | |
| LMTO[d] | +0.215 | +0.035 | −0.005 | | | |
| PP[e] | | | | +0.333 | +0.024 | −0.042 |
| TB[f] | +0.166 | +0.013 | +0.004 | | | |

[a]Present work; PBE calculations.
[b]Reference 23; LDA calculations.
[c]Reference 21; GGA calculations.
[d]Reference 12; LDA calculations.
[e]Reference 13; LDA calculations.
[f]Reference 25.

ideal values than higher cutoff energies, e.g., 18.06 Ry (used in the present work).

### B. Effective pair potentials

To identify further trends in our surface energy data base, we calculate the effective pair-potential (EPP) parameters using the model suggested by Vitos *et al.*,[21] which relates the EPP parameters with the surface energies and coordination changes by the following equation:

$$E_{\mathrm{surf}}(hkl) = \sum_{s=1}^{N_s} n_s(hkl) V_s. \tag{3}$$

In Eq. (3), $n_s(hkl)$ is the number of broken pair bonds in the $s$th coordination shell for a surface of index $(hkl)$, while $N_s$ is the number of coordination shells included in the expansion. Vitos *et al.*[21] suggested that three-body (and higher) interactions is expected to play a role only for early transition metals, which is not the case of Cu, hence such interactions were not included in the expansions. In the present work, we restricted ourselves to the first three EPP parameters, i.e., $V_1$, $V_2$, and $V_3$, however, it should be pointed out that $V_4$ or higher EPP parameters cannot be determined using our surface energy data base because the expansions for the studied high-Miller-index surfaces are linear combinations of the expansions of the low-Miller-index surfaces (see the Appendix). The EPP model is based on a pair-potential expansion of the energy on a fixed lattice, however, we have used the same approach for the relaxed Cu surfaces. The effective parameters $V_1$, $V_2$, $V_3$ obtained from the relaxed flat surfaces are taking into account the relaxation in an average manner. The EPP parameters calculated using the surface energies of (111), (100), and (110) reported in Table III are summarized in Table V along with previously published results.

We found that $V_1^f$ and $V_1$ are smaller than the average surface energy of the low-Miller-index Cu surfaces per number broken nearest-neighbor bonds by 2.0% and 14.0%, respectively. Furthermore, we obtained that $V_1^f/V_2^f \approx 16$, $V_1^f/V_3^f \approx -163$, $V_2^f/V_3^f \approx -10$, while $V_1/V_2 \approx 12$, $V_1/V_3 \approx 37$, $V_2/V_3 \approx 3$. Thus we can conclude that the second and third EPP parameters play a larger role for the relaxed surfaces than for the unrelaxed surfaces, which is expected due to the larger deviation of the broken bond rule for the fully relaxed surfaces.

Using the EPP parameters reported in Table V and the EPP expansions reported in the Appendix we calculated the surface energy of the studied vicinal Cu surfaces. Hence the accuracy of these results can be checked with our FLAPW results reported in Table III. All surface energies calculated using the EPP parameters are summarized in Table VI. Our EPP surface energies for the unrelaxed (relaxed) high-Miller-index Cu surfaces differ less than 1.0% (0.60%) compared to the calculated surface energies. Hence we can conclude that the EPP model can be used to obtain the surface energy of different high-Miller-index surfaces with errors smaller than 1.0% compared with first-principles calculations assuming that the surface energies of the low-Miller-index surfaces are well converged with respect to the computational parameters. Furthermore, the energy gain due to the multilayer relaxations calculated from the EPP surface energies, i.e., $E_{\mathrm{surf}}^{\mathrm{EPP,f}} - E_{\mathrm{surf}}^{\mathrm{EPP}}$, differs from the FLAPW results by almost 20% at the average.

### C. Step energies

The step energy per unit step length of a vicinal surface with a periodic succession of terraces with equal widths, separated by steps of monoatomic height, can be calculated using the following equation:[46,25]

$$E_{\mathrm{step}}(p) = E_{\mathrm{surf}}(p) - (p - 1 + f) E_{\mathrm{surf}}(\infty), \tag{4}$$

where $E_{\mathrm{surf}}(p)$ is the surface energy per surface atom of a vicinal surface with orientation $(hkl)$. $p$ characterizes the number of atom rows (including the inner edge) parallel to the step edge in the terrace, while $f$ is a geometrical factor

TABLE VI. Surface energy of Cu surfaces calculated using the EPP parameters. $\Delta E_{surf}^{EPP}$ indicates the energy gain due to the multilayer relaxations, i.e., $\Delta E_{surf}^{EPP}=E_{surf}^{EPP,f}-E_{surf}^{EPP}$. The numbers in parentheses indicate the relative error with respect to the FLAPW results in Table III.

| Surface | $E_{surf}^{EPP,f}$ (eV) | | $E_{surf}^{EPP}$ (eV) | | $\Delta E_{surf}^{EPP}$ (meV) | |
|---|---|---|---|---|---|---|
| Cu(111) | 0.470 | (0.00%) | 0.469 | (0.00%) | 0.97 | (0.00%) |
| Cu(100) | 0.608 | (0.00%) | 0.603 | (0.00%) | 5.24 | (0.00%) |
| Cu(110) | 0.925 | (0.00%) | 0.901 | (0.00%) | 23.67 | (0.00%) |
| Cu(311) | 1.082 | (−0.99%) | 1.058 | (−0.46%) | 23.99 | (−19.91%) |
| Cu(331) | 1.395 | (−0.19%) | 1.370 | (+0.42%) | 24.64 | (−27.60%) |
| Cu(210) | 1.537 | (−0.29%) | 1.490 | (−0.13%) | 46.70 | (−5.20%) |
| Cu(211) | 1.552 | (−0.49%) | 1.527 | (+0.16%) | 24.96 | (−28.86%) |
| Cu(511) | 1.690 | (−0.15%) | 1.661 | (+0.47%) | 29.23 | (−25.88%) |
| Cu(221) | 1.865 | (+0.07%) | 1.839 | (+0.60%) | 25.61 | (−27.45%) |
| Cu(711) | 2.298 | (−0.33%) | 2.264 | (+0.12%) | 34.47 | (−23.28%) |
| Cu(320) | 2.462 | (+0.15%) | 2.392 | (+0.15%) | 70.37 | (+0.21%) |
| Cu(553) | 2.335 | (−0.20%) | 2.308 | (+0.38%) | 26.57 | (−33.58%) |
| Cu(410) | 2.753 | (−0.04%) | 2.696 | (+0.32%) | 57.17 | (−14.70%) |
| Cu(911) | 2.906 | (−0.75%) | 2.867 | (−0.35%) | 39.71 | (−22.99%) |
| Cu(332) | 2.805 | (−0.05%) | 2.777 | (+0.44%) | 27.54 | (−32.87%) |

depending on the vicinal surface. The parameters $p$ and $f$ are summarized in Tables I and VII, respectively. $E_{surf}(\infty)$ is the surface energy per surface atom of the terrace surface, which can be (111), (100), (110). The value of the step energy for an isolated step is then obtained in the limit of large values of $p$. Consequently, the nature and order of magnitude of the step-step interactions can be inferred from the study of $E_{step}(p)$ as a function of the values of $p$. In the present work, the step energies were calculated for unrelaxed and fully relaxed slabs, which are indicated by $E_{step}^{f}$ and $E_{step}$, respectively.

For the particular case of the vicinal Cu$(2p-1,11)$ surfaces, for which there are available experimental results,[10] we calculated the step-step interactions for $p=2$, 3, 4, and 5 (different terrace widths). The results are plotted in Fig. 2. As expected the multilayer relaxations decreases the step energies but the step energies show the same trend as a function of the number of atom-rows in the terrace for unrelaxed and fully relaxed slabs. The minimum obtained for $p=3$ reveals a relative attraction between the steps for short terraces, e.g., for $p=3$, 4 and $p=5$. This result is in agreement with scanning tunneling microscope[10] results, which found an attrac-

TABLE VII. Step energies of isolated steps given in electron volts per surface atom for various vicinal Cu geometries calculated from the FLAPW surface energies (surfaces with the largest terraces) and the EPP parameters.

| | $(p,p,p-2)$<br>$p(111)\times(11\bar{1})$<br>$f=1/3$<br>$2V_1+4V_3$ | $(2p-1,11)$<br>$p(100)\times(111)$<br>$f=1/2$<br>$V_1+2V_2$ | $(p-1,1,0)$<br>$p(100)\times(110)$<br>$f=0$<br>$2V_1+2V_2$ | $(2p-1,2p-1,1)$<br>$p(110)\times(111)$<br>$f=1/2$<br>$V_2+2V_3$ | $(p,p-1,0)$<br>$p(110)\times(100)$<br>$f=1/2$<br>$V_1+2V_3$ | $(2p-3,2p-1,1)$<br>$p(110)\times(\bar{1}11)$<br>$f=0$<br>$V_1+V_2+2V_3$ |
|---|---|---|---|---|---|---|
| FLAPW[a] | 0.300 | 0.192 | 0.322 | 0.010 | 0.146 | |
| FLAPW[b] | 0.264 | 0.164 | 0.276 | 0.012 | 0.134 | |
| EPP[a] | 0.299 | 0.170 | 0.321 | 0.007 | 0.149 | 0.158 |
| EPP[b] | 0.276 | 0.153 | 0.284 | 0.018 | 0.138 | 0.149 |
| LMTO[c] | 0.380 | 0.200 | 0.363 | 0.046 | 0.190 | 0.209 |
| TB[d] | 0.348 | 0.192 | 0.358 | 0.021 | 0.174 | 0.187 |
| FKKR[e] | 0.438 | 0.249 | 0.474 | 0.006 | 0.219 | 0.231 |
| PP[f] | 0.497 | 0.382 | 0.715 | −0.061 | 0.248 | 0.272 |

[a]Present work using the FLAPW surface energies (EPP parameters) from unrelaxed slabs.
[b]Present work using the FLAPW surface energies (EPP parameters) from fully relaxed slabs.
[c]Reference 21 (unrelaxed slabs).
[d]Reference 25 and 26 (unrelaxed slabs).
[e]Reference 23.
[f]Reference 13.

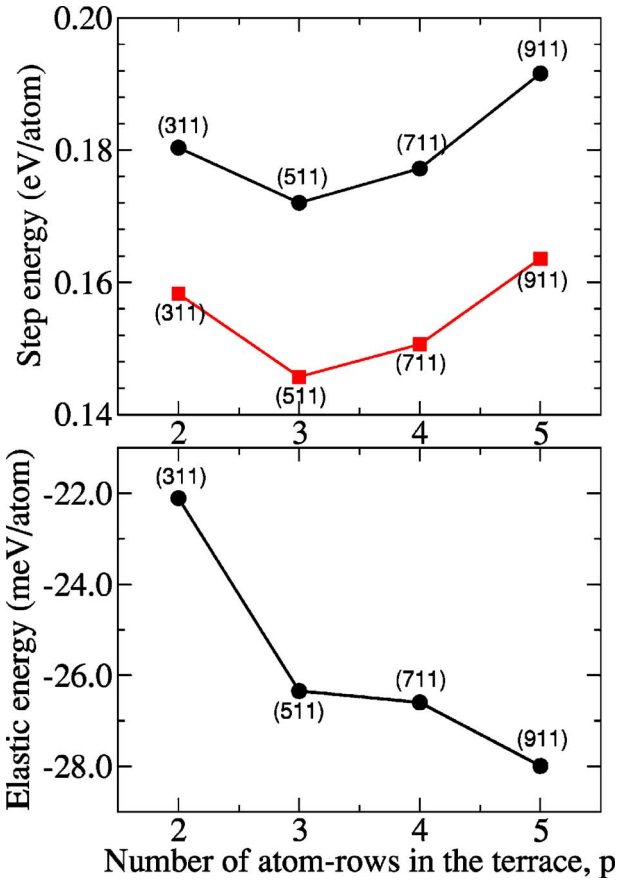


FIG. 2. (Color online) (a) Step energies per atom as function of the number of atom rows in the terraces for the stepped Cu($2n-1,11$) surfaces. Circles (in black) and squares (in red) indicate step energies obtained from unrelaxed and fully relaxed surfaces, respectively. (b) Elastic energy calculated as $E^{f}_{\mathrm{step}}-E_{\mathrm{step}}$ for different surfaces. The straight lines are only a guide for the eyes.

tive interaction at intermediate terrace distances ($p=4$ and 5). Unfortunately one could not reach large enough terraces to obtain a clear convergence of the step energy towards the asymptotic value of an isolated step. One would probably need to go up to $p=8$ or even $p=9$ which requires a very large computer time. Interestingly one can note that the usual repulsive elastic step-step interaction is buried in a dominant Friedel like electronic interaction. An evaluation of the elastic interaction can be obtained by writing the relaxed step energy $E_{\mathrm{step}}$ as the sum of the unrelaxed step energy $E^{f}_{\mathrm{step}}$ plus an extra negative term $\Delta_{\mathrm{relax}}(p)$ gained during the relaxation process (see Fig. 2). This term itself depends on the terrace width and its variation is of 6 meV between $p=2$ and $p=5$ which is a very reasonable estimation of the strength for the elastic interaction.

Using our FLAPW surface energies for the vicinal surfaces with the largest terrace widths, we calculated the step-step interactions for different vicinal orientations. The results are summarized in Table VII. For all studied cases, except for $p(110)\times(111)$ vicinal, the multilayer relaxations decreases the step-step interaction. We found the following trend: $E^{p(100)\times(110)}_{\mathrm{step}} > E^{p(111)\times(111)}_{\mathrm{step}} > E^{p(100)\times(111)}_{\mathrm{step}} > E^{p(110)\times(010)}_{\mathrm{step}} > E^{p(110)\times(111)}_{\mathrm{step}}$, which is agreement with previous theoretical results.[25]

Using the EPP model the energy of isolated steps can be expressed as

$$E_{\mathrm{step}}(p)=\sum_{s=1}^{N_s} n_{\mathrm{step},s}(p)V_s, \tag{5}$$

where $n_{\mathrm{step},s}=n_s(p)-(p-1+f)n_s(\infty)$.[26] The numbers $n_s(p)$ and $n_s(\infty)$ are the total number of bonds in the $s$th coordination sphere broken by the vicinal and flat surfaces, respectively. Due to the short range of the EPP parameters, $n_{\mathrm{step},s}$ becomes a constant as soon as $p$ overcomes a value $p_\infty$, which is usually very small: most often, according to Vitos *et al.*,[21] $p_\infty=2$. For example, the step energies for the Cu($2p-1,11$) surface calculated using Eq. (4) and the relations in the Appendix do not depend on the number of atom rows in the terrace, i.e., $E_{\mathrm{step}}(p)=V_1+2V_2$ for $p=2,3,4,5,\ldots$. Therefore differences of less than 1.0% between the calculated surface energies and the EPP surfaces energies determines the dependence of the step energies as a function of the terrace widths. Using Eq. (5), we calculated the step-step energy interaction of isolated steps corresponding to stepped surfaces with either (111), (100), or (110) terraces. The results are summarized in Table VII along with previous results.

Using our FLAPW surface energies we found stepped energies of 0.192 and 0.163 eV for the unrelaxed and relaxed Cu(911) surfaces, respectively, which we *assumed* that can be compared with the step energies of isolated steps calculated using the EPP model. Using the EPP parameters, we obtained 0.170 eV and 0.153 eV, for the unrelaxed and fully relaxed surfaces, respectively. Thus the EPP model provide step energies smaller by $\approx$11.0% ($\approx$6.0%) for the unrelaxed (fully relaxed) slabs. For the vicinal $p(111)\times(111)$ surfaces the results obtained using the FLAPW surface energies and the EPP parameters differs by 0.35% and 4.5% for unrelaxed and relaxed surfaces, respectively. In general, we can conclude that the step energies of isolated steps can be estimated using the EPP parameters.

### D. Stability of vicinal Cu surfaces at 0 K

Vicinal surfaces are not always stable. The surface energy per unit area of a vicinal surface is large and it might be energetically favorable for a solid to expose to the vacuum region low-Miller-index facets which has smaller surface energies per area (see Table III), even if the total surface area is increased by the transformation. In the present work, we will follow the approach suggested by Desjonquéres *et al.*,[22] which is described in detail in Ref. 25, to study the stability of the vicinal (100) and (111) Cu surfaces with respect to faceting. According to the formulation proposed by Desjonquères and co-workers[22,25] a vicinal surface of the (111)-(100) domain is stable (unstable) with respect to faceting into (100) and (111) facets, if $\Delta f(\tan\theta)<0$ [$\Delta f(\tan\theta)>0$]. $\Delta f(\tan\theta)$ is given by the following equation:

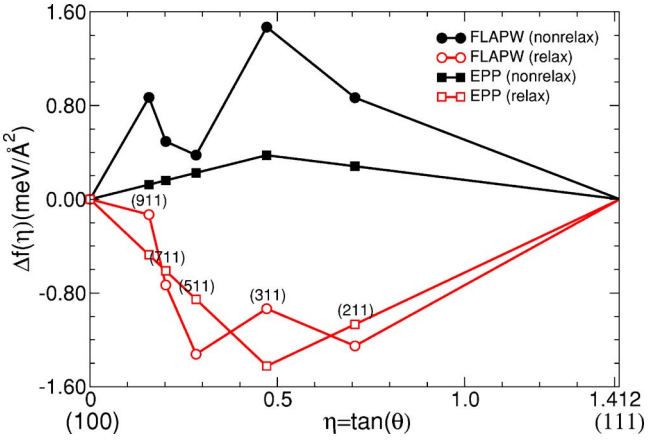


FIG. 3. (Color online) Stability function $\Delta f(\eta)$ with respect to faceting into (100) and (111) facets at zero temperature for Cu surfaces calculated from FLAPW and EPP surface energies. The surface energies were calculated with and without relaxations of the slab. The lines are only guide for the eyes.

$$\Delta f(\tan(\theta)) = [E_{\text{surf}}(hkl) - (p-1)E_{\text{surf}}(100) - E_{\text{surf}}(111)]/A_0(hkl), \quad \text{for } p(100)\times(111) \text{ and} \tag{6}$$

$$\Delta f(\tan(\theta)) = [E_{\text{surf}}(hkl) - E_{\text{surf}}(100) - (p-1)E_{\text{surf}}(111)]/A_0(hkl), \quad \text{for } p(111)\times(100). \tag{7}$$

The surface energies in the equations above are in electron volt per surface atom. $\theta$ is the angle between the normals to the vicinal $(hkl)$ surfaces and the reference orientation (100). $\tan(\theta)=\sqrt{2}/(2p-1)$ for $p(100)\times(111)$ and $4\sqrt{2}/(3p-1)$ for $p(111)\times(100)$, where $p$ is the number of atom-rows in the terraces. $A_0(hkl)=A\cos(\theta)$, i.e., $A_0(hkl)$ is the area of the projection of the surface unit cell area of the vicinal surface, $A$, on the (100) plane. It can easily show that $A_0(hkl)=\cos(\theta)\sqrt{(2p-1)^2+2}a_0^2/4$ for stepped $p(100)\times(111)$ surfaces and $A_0(hkl)=\cos(\theta)\sqrt{(p+1)^2+2(p-1)^2}a_0^2/4$ for $p(111)\times(100)$.

As a first test, we calculated $\Delta f(\tan\theta)$ for (311). We found for all test calculations using different number of layers in the slab for the (311), (100), and (111) surfaces that $\Delta f(\tan\theta)>0$ ($<0$) for unrelaxed (fully relaxed) slabs. Thus our results are converged with respect to the number of layers in the slab. Using our FLAPW surface energies we calculated the stability function, $\Delta f(\tan\theta)$, for the unrelaxed and fully relaxed vicinal surfaces of the type $p(100)\times(111)$ and $p(111)\times(100)$, which is plotted in Fig. 3. Furthermore, we calculated the stability function using also the EPP surface energies.

We found that all unrelaxed (fully relaxed) vicinal Cu surfaces of the type $p(100)\times(111)$ and $p(111)\times(100)$ are unstable (stable), i.e., $\Delta f(\tan\theta)>0$ ($<0$), with respect to faceting into (100) and (111) facets at zero temperature. It can be observed in Fig. 3 for the fully relaxed surfaces two local minimum at the (511) and (211) surfaces, which should lead to an unstable (311) surface. However, we want to point out that the energy balance is so delicate that numerical errors cannot be excluded. Apart from this questionable oscillating feature, our results are in agreement with experimental results, which observed that the vicinal surfaces are stable at room temperature. Therefore our results clearly indicate that the multilayer relaxations of the vicinal surfaces play an essential role in the stability of the vicinal surfaces with respect to faceting, which was not obtained in previous semiempirical studies. This finding is very interesting since it shows that (100)-(111) vicinal Cu surfaces are at the verge of (in)stability and are very sensitive to elastic interactions. This may be explained by the tendency to develop facets under deposition of adsorbates like silver atoms.[45]

Furthermore, the same conclusions with respect to the stability of the vicinal surfaces are obtained also using the EPP surface energies. Thus our results suggest that the combination of high quality first-principles calculations for low-Miller-index surfaces and the EPP model can provide a better understanding of the stability of vicinal surfaces. However, we cannot exclude that the good agreement between the EPP and FLAPW results for the stability of the vicinal surfaces is a fortuitous result and particular for Copper surfaces due to the delicate balance between the surface energies of the different Cu surfaces.

## IV. SUMMARY

In the present work we calculated the surface energy of unrelaxed and fully relaxed low- and high-Miller-index Cu surfaces employing the all-electron FLAPW method to solve the Kohn-Sham equations. The following 15 Cu surfaces were studied: (111), (100), (110), (311), (331), (211), (210), (511), (221), (320), (711), (553), (410), (911), and (332).

We found that the unrelaxed vicinal $p(100)\times(111)$ and $p(111)\times(100)$ Cu surfaces are unstable relative to faceting at 0 K, while the fully relaxed vicinal Cu surfaces are stable relative to faceting, which is in agreement with the observed stability of vicinal Cu surfaces at room temperature. Therefore the multilayer relaxations of the vicinal Cu surfaces play an important role in the stability of the mentioned surfaces with respect to faceting.

Concerning the step-step interactions for the vicinal Cu surfaces of the type $p(100)\times(111)$, we obtained a minimum for $p=3$, which reveals a relative attraction between the steps for short terraces, e.g., for $p=3$, 4 and $p=5$. This result is in agreement with STM (Ref. 10) results, which obtained an attractive interaction at intermediate terrace distances ($p=4$ and 5).

We obtained that the surface energies of the unrelaxed and fully relaxed Cu surfaces studied in the present work can be calculated using the EPP approach and the surface energies of the unrelaxed and fully relaxed low-Miller-index Cu surfaces, respectively, with errors smaller than 1.0% compared with the calculated FLAPW surface energies. This finding is a consequence of the *almost perfect* linear scaling of the surface energy of the Cu surfaces as a function of the total number of broken nearest-neighbor bonds in the Cu$(hkl)$ sur-

faces. Using the surface energies derived from the EPP model, we found the same conclusion concerning the stability of the vicinal $p(100)\times(111)$ and $p(111)\times(100)$ Cu surfaces surfaces with respect faceting at 0 K. Therefore we conclude in the present work that high accurate first-principles calculations for low-Miller-index surfaces combined with the EPP model can provide insights in the energetics of vicinal surfaces.

## APPENDIX

Using the EPP expansions [Eq. (3)] within $N_s=4$ and the number of broken pair bonds in the $s$th coordination shell for the studied unrelaxed Cu($hkl$) surfaces, we found the following set of relations:

$$E_{\mathrm{surf}}(111) = 3V_1 + 3V_2 + 12V_3 + 6V_4, \quad \text{(A1)}$$

$$E_{\mathrm{surf}}(100) = 4V_1 + 2V_2 + 16V_3 + 8V_4, \quad \text{(A2)}$$

$$E_{\mathrm{surf}}(110) = 6V_1 + 4V_2 + 20V_3 + 12V_4, \quad \text{(A3)}$$

$$E_{\mathrm{surf}}(311) = 7V_1 + 5V_2 + 24V_3 + 14V_4, \quad \text{(A4)}$$

$$E_{\mathrm{surf}}(331) = 9V_1 + 7V_2 + 32V_3 + 18V_4, \quad \text{(A5)}$$

$$E_{\mathrm{surf}}(210) = 10V_1 + 6V_2 + 32V_3 + 20V_4, \quad \text{(A6)}$$

$$E_{\mathrm{surf}}(211) = 10V_1 + 8V_2 + 36V_3 + 20V_4, \quad \text{(A7)}$$

$$E_{\mathrm{surf}}(511) = 11V_1 + 7V_2 + 40V_3 + 22V_4, \quad \text{(A8)}$$

$$E_{\mathrm{surf}}(221) = 12V_1 + 10V_2 + 44V_3 + 24V_4, \quad \text{(A9)}$$

$$E_{\mathrm{surf}}(711) = 15V_1 + 9V_2 + 56V_3 + 30V_4, \quad \text{(A10)}$$

$$E_{\mathrm{surf}}(320) = 16V_1 + 10V_2 + 52V_3 + 32V_4, \quad \text{(A11)}$$

$$E_{\mathrm{surf}}(553) = 15V_1 + 13V_2 + 56V_3 + 30V_4, \quad \text{(A12)}$$

$$E_{\mathrm{surf}}(410) = 18V_1 + 10V_2 + 64V_3 + 36V_4, \quad \text{(A13)}$$

$$E_{\mathrm{surf}}(911) = 19V_1 + 11V_2 + 72V_3 + 38V_4, \quad \text{(A14)}$$

$$E_{\mathrm{surf}}(332) = 18V_1 + 16V_2 + 68V_3 + 36V_4, \quad \text{(A15)}$$

where the coefficients of $V_1$, $V_2$, $V_3$, and $V_4$ indicate the total number of broken first-, second-, third-, and fourth-neighbor bonds, respectively. It can be shown from the equations above that the EPP expansions for the studied high-Miller-index surfaces can be written as a linear combination of the expansions of the low-Miller-index surfaces. Thus we cannot determine the $V_4$ parameter from our surface energy data base. Therefore we restricted ourselves to the first three EPP parameters, which can be determined using the surface energy of the low-Miller-index surfaces. We set $V_4, V_5, V_6, \ldots V_s=0$. From the equations for the low-Miller-index surfaces, we found the following relations:

$$V_1 = E_{\mathrm{surf}}(110) - E_{\mathrm{surf}}(111) - E_{\mathrm{surf}}(100)/2, \quad \text{(A16)}$$

$$V_2 = 2E_{\mathrm{surf}}(111)/3 - E_{\mathrm{surf}}(100)/2, \quad \text{(A17)}$$

$$V_3 = E_{\mathrm{surf}}(111)/6 + E_{\mathrm{surf}}(100)/4 - E_{\mathrm{surf}}(110)/4. \quad \text{(A18)}$$

The following set of EPP parameters were obtained: $V_1^f = +0.151\,163$ eV, $V_2^f = +0.009\,193$ eV, and $V_3^f = -0.000\,929$ eV for unrelaxed surfaces, while for fully relaxed surfaces we obtained $V_1 = +0.131\,079$ eV, $V_2 = +0.011\,167$ eV, and $V_3 = +0.003\,518$ eV. Thus using the EPP parameters determined from the surface energy of the low-Miller-index surfaces and the Eqs. (A4)–(A15), we can calculate the surface energies for all high-Miller-index Cu surfaces and compare it with our FLAPW results. Thus errors in the EPP model in obtaining surface energies of high-Miller-index surfaces can be discussed in detail.

*Present address: Humboldt-Universitaet zu Berlin, Institut fuer Chemie Arbeitsgruppe Quantenchemie, Unter den Linden 6, D-10099 Berlin, Germany. Email address: dasilvaj@chemie.huberlin.de

[1] M. C. Desjonquères and D. Spanjaard, *Concepts in Surface Science* (Springer, New York, 1995).
[2] J. J. Métois and P. Müller, Surf. Sci. **548**, 13 (2004).
[3] H. P. Bonzel and A. Emundts, Phys. Rev. Lett. **84**, 5804 (2000).
[4] C. Bombis, A. Emundts, M. Nowicki, and H. P. Bonzel, Surf. Sci. **511**, 83 (2002).
[5] H. P. Bonzel and M. Nowicki, Phys. Rev. B **70**, 245430 (2004).
[6] M. Nowicki, C. Bombis, A. Emundts, H. P. Bonzel, and P. Wynblatt, Europhys. Lett. **59**, 239 (2002).
[7] M. Nowicki, C. Bombis, A. Emundts, and H. P. Bonzel, Phys. Rev. B **67**, 075405 (2003).
[8] W. R. Tyson and W. A. Miller, Surf. Sci. **62**, 267 (1977).
[9] F. R. de Boer, R. Boom, W. C. M. Mattens, A. R. Miedema, and A. K. Niessen, *Cohesion in Metals* (North-Holland, Amsterdam, 1988).
[10] J. Frohn, M. Giesen, M. Poensgen, J. F. Wolf, and H. Ibach, Phys. Rev. Lett. **67**, 3543 (1991).
[11] M. Methfessel, D. Hennig, and M. Scheffler, Phys. Rev. B **46**, 4816 (1992).
[12] H. L. Skriver and N. M. Rosengaard, Phys. Rev. B **46**, 7157 (1992).
[13] Th. Rodach, K.-P. Bohnen and K. M. Ho, Surf. Sci. **286**, 66 (1993).
[14] Z.-J. Tian and T. S. Rahman, Phys. Rev. B **47**, 9751 (1993).
[15] S. Wei and M. Y. Chou, Phys. Rev. B **50**, 4859 (1994).
[16] P. J. Feibelman, Phys. Rev. B **52**, 16845 (1995).
[17] S. Papadia, M. C. Desjonquères, and D. Spanjaard, Phys. Rev. B **53**, 4083 (1996).

[18] G. Boisvert, L. J. Lewis, and M. Scheffler, Phys. Rev. B **57**, 1881 (1998).
[19] L. Vitos, A. V. Ruban, H. L. Skriver, and J. Kollár, Surf. Sci. **411**, 186 (1998).
[20] J. W. M. Frenken and P. Stoltze, Phys. Rev. Lett. **82**, 3500 (1999).
[21] L. Vitos, H. L. Skriver, and J. Kollár, Surf. Sci. **425**, 212 (1999).
[22] M. C. Desjonquères, D. Spanjaard, C. Barreteau, and F. Raouafi, Phys. Rev. Lett. **88**, 056104 (2002).
[23] I. Galanakis, G. Bihlmayer, V. Bellini, N. Papanikolaou, R. Zeller, S. Blügel, and P. H. Dederichs, Europhys. Lett. **58**, 751 (2002).
[24] I. Galanakis, N. Papanikolaou, and P. H. Dederichs, Surf. Sci. **511**, 1 (2002).
[25] F. Raouafi, C. Barreteau, M. C. Desjonquères, and D. Spanjaard, Surf. Sci. **505**, 183 (2002).
[26] C. Barreteau, F. Raoufi, M. C. Desjonquères, and D. Spanjaard, J. Phys.: Condens. Matter **15**, S3171 (2003).
[27] J. L. F. Da Silva, Phys. Rev. B **71**, 195416 (2005).
[28] P. Hohenberg and W. Kohn, Phys. Rev. **136**, B864 (1964).
[29] W. Kohn and L. J. Sham, Phys. Rev. **140**, A1133 (1965).
[30] J. P. Perdew, K. Burke, and M. Ernzerhof, Phys. Rev. Lett. **77**, 3865 (1996).
[31] D. J. Singh, *Plane Waves, Pseudopotentials and LAPW Method* (Kluwer Academic Publishers, Boston, 1994).
[32] http:www.flapw.de
[33] H. Krakauer, M. Posternak, and A. J. Freeman, Phys. Rev. B **19**, 1706 (1979).
[34] In the present work a higher cutoff energy and a larger number of **k** points were used compared to the multilayer relaxation studies reported in Refs. 40–42 due to the high accuracy required to the study of the stability of vicinal Cu surfaces and step energies. All slabs optimized in Refs. 40–42 were optimized again using the computational parameters reported in the present work.
[35] H. J. Monkhorst and J. D. Pack, Phys. Rev. B **13**, 5188 (1976).
[36] M. G. Gillan, J. Phys.: Condens. Matter **1**, 689 (1989).
[37] C. Kittel, in *Introduction to Solid State Physics*, 7th ed. (Wiley, New York, 1996).
[38] J. L. F. Da Silva, Ph.D. thesis, Technical University Berlin, Berlin, 2002.
[39] B. Lang, R. W. Joyner, and G. A. Somorjai, Surf. Sci. **30**, 440 (1972).
[40] J. L. F. Da Silva, K. Schroeder, and S. Blügel, Phys. Rev. B **69**, 245411 (2004).
[41] J. L. F. Da Silva, K. Schroeder, and S. Blügel, Phys. Rev. B **70**, 245432 (2004).
[42] J. L. F. Da Silva, K. Schroeder, and S. Blügel, Phys. Rev. B **72**, 033405 (2005).
[43] V. Fiorentini and M. Methfessel, J. Phys.: Condens. Matter **8**, 6525 (1996).
[44] P. Blaha, K. Schwarz, and J. Luitz, WIEN97, A Full-Potential Linearized Augmented Plane Wave Package for Calculating Crystal Properties (Karlheinz Schwarz, Techn. Univ. Wien, Vienna, 1999). ISBN 3-9501031-0-4, Updated version of P. Blaha, K. Schwarz, P. Sorantin, and S. B. Trickey, Comput. Phys. Commun. **59**, 399 (1990).
[45] A. R. Bachmann, A. Mugarza, J. E. Ortega, and S. Speller, Phys. Rev. B **64**, 153409 (2001).
[46] F. Ducastelle, J. Phys. (France) **31**, 1055 (1970).